

Moiré-like superlattice generated van Hove singularities in strained CuO_2 double layer

A.O. Sboychakov,¹ K.I. Kugel,^{1,2} and A. Bianconi^{3,4,5}

¹*Institute for Theoretical and Applied Electrodynamics,
Russian Academy of Sciences, 125412 Moscow, Russia*

²*Institute of Metal Physics, Ural Branch, Russian Academy of Sciences, 620990 Ekaterinburg, Russia*

³*Rome International Center for Materials Science Superstripes RICMASS, via dei Sabelli 119A, 00185 Rome, Italy*

⁴*Institute of Crystallography, CNR, Via Salaria Km 29.300, 00015 Monterotondo Rome, Italy*

⁵*National Research Nuclear University, MEPhI (Moscow Engineering
Physics Institute), Kashirskoe sh. 31, 115409 Moscow, Russia*

(Dated: February 4, 2022)

While it is known that the double-layer $\text{Bi}_2\text{Sr}_2\text{CaCu}_2\text{O}_{8+y}$ (BSCCO) cuprate superconductor exhibits an incommensurate superlattice (IS), the effect of IS on the electronic structure remains elusive. The interlayer interaction produces a double-peaked van Hove singularity (VHS) in the density of states (called bilayer splitting) which is strongly changed by the incommensurate period of the superlattice controlled by the misfit strain between different atomic layers in BSCCO. Recently the wave vector $\mathbf{q} = \epsilon \mathbf{b}$ (where \mathbf{b} is the reciprocal lattice vector of the average lattice) of the superlattice in a high-quality single crystal has been measured with high precision [N. Poccia *et al.*, Phys. Rev. Materials **4**, 114007 (2020)]. This work reports the calculation of the VHS bilayer splitting in a *quasi-commensurate* phase with a rational number $\epsilon = 9/43$ for the pure BSCCO crystal. We extend the calculation to the devil's staircase observed in the high entropy perovskite $\text{Bi}_2\text{Sr}_2\text{Ca}_{1-x}\text{Y}_x\text{Cu}_2\text{O}_{8+y}$ (BSCYCO), where the wave vector $\epsilon = 9/\eta$ changes in the range $36 > \eta > 43$ for $1 > x > 0$ controlled by the lattice misfit strain. Our results are of high relevance where the chemical potential is tuned in the optimum and overdoped regime where the superconductor to metal transition takes place. The similarity of the complex VHS splitting due to the devil's staircase in mismatched CuO_2 bilayer with VHS due to moiré lattice in strained twisted graphene. This makes mismatched CuO_2 bilayer quite promising for constructing quantum devices with tuned physical characteristics.

PACS numbers: 73.20.At

I. INTRODUCTION

Different van der Waals heterostructures¹, such as bilayer graphene² and transition metal dichalcogenide bilayers^{3,4} provide an actively progressing testing ground for a variety of quantum phenomena, e.g., flat bands, electron nematicity, etc. Indeed, if we put together two layers of van der Waals materials, a lattice mismatch or twist angle lead to the formation of moiré patterns with large supercells. This provides a promising means of the band and crystal structure engineering leading, in particular, to the moiré modulated topological order⁵, and paving way to such novel field of research as twistronics⁶.

Bilayers of atomic cuprate oxide superconductors appear to be not less interesting. While the lattice parameter and aperiodic local lattice distortions associated with variable microstrain are not a key physical parameter either in BCS and unconventional superconductivity theories, a compelling evidence for the key role of CuO_2 lattice in the mechanism of high-temperature superconductivity and charge density wave (CDW) phenomena in cuprate perovskites has been reported^{7–11}. These findings confirm early experimental results provided by local and fast experimental methods based on the use of synchrotron X-ray radiation^{12–16} pointing toward the relevant role of the micro-strain in superconducting cuprate perovskites^{17,18}.

The $\text{Bi}_2\text{Sr}_2\text{CaCu}_2\text{O}_{8+y}$ (BSCCO) crystal^{14–16} is a

misfit layer compound¹⁹ exhibiting an incommensurate composite structure^{19,20} and large atomic displacements from average positions in the $[\text{BiO}]$, $[\text{SrO}]$, $[\text{CuO}_2]$, $[\text{Ca}]$ layers forming an incommensurate composite structure, where a texture of nanoscale insulating and metallic atomic stripes, for example^{21–24} $\text{Bi}_2\text{Sr}_2\text{Ca}_{1-x}\text{Y}_x\text{Cu}_2\text{O}_{8+y}$, (BSCYCO) with six different elements in the average crystalline unit cell forming an archetypal case of High Entropy Perovskites (HEPs). The search of new HEPs is today a hot topic focusing on the manipulation of the complexity, where the entropy control plays a key role in the determination of material functionalities like it is observed in bismuth 2212 iron ferrite and ferrate compounds^{25,26}, thermoelectric misfit layered cobaltite oxide perovskites^{27,28} also in the form of 2D flakes²⁹ taking advantage of the polymorphism of perovskite structure with competing nanoscale crystallographic phases^{30,31}.

Spatially correlated incommensurate lattice stripy modulations in $\text{Bi}_2\text{Sr}_2\text{CaCu}_2\text{O}_{8+y}$ superconductor can now be visualized by the scanning submicron X-ray diffraction focusing on the superlattice satellites of the main X-ray reflections^{32–34}. The results show that, while oxygen concentration and the doping level can change depending on the sample treatments and thermal history, the incommensurate superlattice wavevector is controlled by the misfit strain and it exhibits a remarkable stability. The critical temperature exhibits a dome as a function

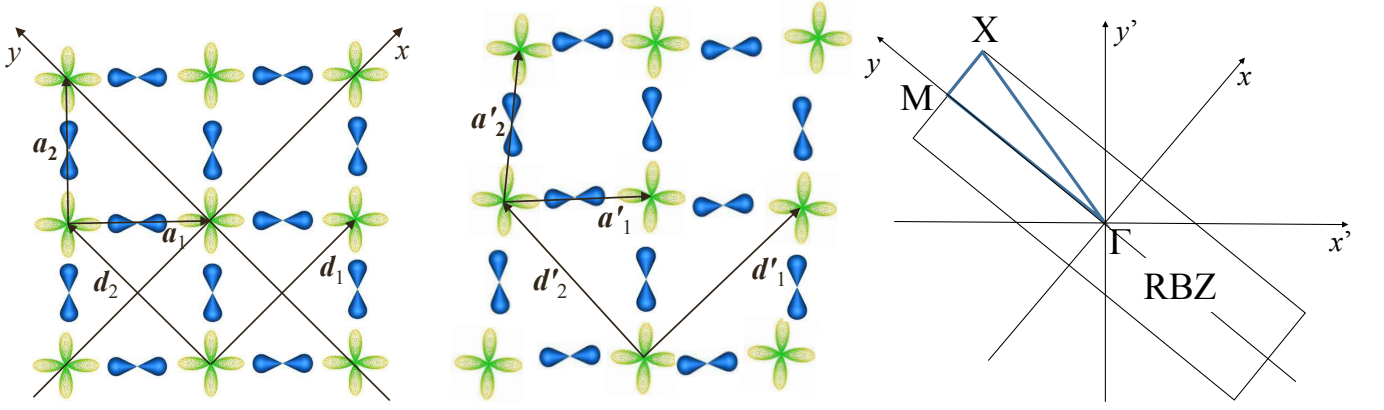


FIG. 1: Schematics of the CuO_2 layer 1 (left panel) and 2 (middle panel). Layer 1 is unstretched. Layer 2 is either stretched or compressed in diagonal (x) direction. As a result, for some commensurate stretching/compression, a superstructure appears. The superlattice contains $2N_1$ elementary unit cells of the layer 1 and $2N_2$ elementary unit cells of the layer 2. Right figure shows the sketch of the reduced Brillouin zone of the superlattice. The Γ point is in the coordinate origin, the M point has coordinates $\mathbf{M} = (0, \pi/d)$, while coordinate of the X point is $\mathbf{X} = (\pi/(N_1d), \pi/d)$. The thick blue triangle shows the contour along which the spectra (see below) are calculated.

of oxygen concentration or by potassium deposition³⁵, but the maximum critical temperature of the dome³⁶ is controlled by the lattice stripe aperiodic structure³⁷ and misfit strain¹⁷.

Recently the scientific interest turned toward the normal state of cuprate perovskites exhibiting high-temperature superconductivity in the overdoped regime in the proximity of the superconductor-to-metal transition tuned by doping, while for many years the focus was on the underdoped regime. The investigations of the overdoped phase^{38–45} of Bi2212 have found evidence that the superconducting gap appearing at temperatures well above the critical temperature T_c , while below T_c a large fraction of the normal state remains uncondensed. Scanning tunneling microscopy has shown that on the edge of the overdoped regime, the gap remains in isolated puddles above T_c , so that superconducting puddles are intercalated by normal metal phase. Moreover, at the same time, the Fermi surface topology changes giving rise to an electronic topological Lifshitz transition providing compelling evidence for a nanoscale phase separation giving a granular landscape, where superconducting puddles are embedded in a normal phase. The phase separation scenario was predicted to appear at the Lifshitz transition several years ago^{46–50}.

In this work, we focus on the variation of the electronic topological transition from a hole Fermi surface to an electron Fermi surface in the overdoped regime in the BSCCO double layer perovskite taking into account the aperiodic incommensurate lattice modulation.

In the BSCCO antiferromagnetic system, $\text{Bi}_2\text{Sr}_2\text{CaCu}_2\text{O}_{8+y}$, the CuO_2 misfit compressive strain is large and the tensile strain in the BiO and SrO rocksalt layers is large, therefore oxygen interstitials mobility is high, and it is possible to add $y = 0.2$ oxygen interstitials to dope the layered perovskite. In

the BSCCO superconducting system $\text{Bi}_2\text{Sr}_2\text{CaCu}_2\text{O}_8$, the CuO_2 misfit compressive strain is small and the tensile strain in the BiO and SrO rocksalt layers is low, therefore the oxygen interstitials mobility is low, and it is not possible to add oxygen interstitials to dope the layered perovskite

The insulating $\text{Bi}_2\text{Sr}_2\text{YCu}_2\text{O}_8$ exhibits a commensurate modulation with $\varepsilon = 0.25$, which indicates the formation of lattice stripes with commensurate period $n = 1/\varepsilon = 4$ lattice units. The superconducting $\text{Bi}_2\text{Sr}_2\text{CaCu}_2\text{O}_{8+y}$ exhibits a commensurate modulation with $\varepsilon = 0.21$, which indicate the formation of lattice stripes superlattice with incommensurate period $n = 1/0.21$ lattice units. For $\varepsilon = 0.2$ the CuO_2 lattice should be decorated by a commensurate stripes superlattice with $n = 1/\varepsilon = 1/0.2 = 5$ lattice units. For intermediate values of the misfit strain and $0.25 < \varepsilon < 0.2$, the incommensurate superstructure⁵¹ consists of the mixture of the $\varepsilon = 1/n$ and $\varepsilon = 1/m$ order, i.e. alternating the so called $n = 4$ stripes portions and $m = 5$ stripes portions. Indeed, quasi-commensurate periods $\lambda = 1/\varepsilon = (nx + my)/(n + m)$ intermediate between two main commensurate wavevectors $1/n$ and $1/m$ with periods of m and n lattice units, respectively, occur at integer numbers of lattice unit cells $\eta = (n + m)/\varepsilon$. Each quasi-commensurate phase (QCP) corresponds to a modulation wave locked with the underline lattice onto a rational number. The sequence of quasi-commensurate phases is called the devil's staircase⁵¹, which have been observed in many complex materials.

The quasi-commensurate modulation period in BSCCO is given by $1/\varepsilon = (4x + 5y)/(4 + 5)$, where $x + y = 9$. Therefore, $\eta = 9/\varepsilon = 4x + 5y$ varies in the range $36 < \eta < 45$ and at each integer value of η the system reaches a quasi-commensurate phase at each step of a *devil's staircase*. We have found that in

the BSCCO samples, where the chemical potential is tuned by the concentration of oxygen interstitials, the mismatched XCuO_2 bilayer is tuned by the misfit strain at the quasi-commensurate modulation with $\eta = 43$ i.e., $\epsilon = 9/43 = 0.209$ in agreement with the recent scanning micro-X-ray diffraction³⁴ which is the *devil's staircase* for $x = 2$ and $y = 5$, therefore we have $4 \times 2 + 5 \times 7 = 43$ (i.e. a quasicrystal made of 8 insulating lattice units and 35 metallic lattice units).

II. GEOMETRY OF THE SYSTEM

We model the system under study as consisting of two mismatched CuO_2 layers. The layer 1 is assumed to be quadratic. For the reason described below, we choose the reference frame as shown on the left panel in Fig. 1. For such a choice, the vectors connecting next nearest-neighbor Cu ions have coordinates $\mathbf{d}_1 = d(1, 0)$ and $\mathbf{d}_2 = d(0, 1)$, where d is the distance between nearest copper ions in the *diagonal* direction. We choose $d = 5.37 \text{ \AA}$. We also introduce vectors connecting nearest-neighbor Cu ions of the layer 1 (lattice vectors of the unit cell of layer 1). They are expressed via vectors $\mathbf{d}_{1,2}$ according to $\mathbf{a}_1 = (\mathbf{d}_1 - \mathbf{d}_2)/2$ and $\mathbf{a}_2 = (\mathbf{d}_1 + \mathbf{d}_2)/2$. The positions of Cu ions in the layer 1 are

$$\mathbf{r}_{1\mathbf{n}}^d \equiv \mathbf{r}_{1\mathbf{n}} = n\mathbf{a}_1 + m\mathbf{a}_2, \quad (1)$$

where $\mathbf{n} = (n, m)$ (n, m are integers), while the positions of oxygen ions are

$$\mathbf{r}_{1\mathbf{n}}^{p_x} = \mathbf{r}_{1\mathbf{n}} + \frac{1}{2}\mathbf{a}_1, \quad \mathbf{r}_{1\mathbf{n}}^{p_y} = \mathbf{r}_{1\mathbf{n}} + \frac{1}{2}\mathbf{a}_2. \quad (2)$$

Layer 2 is assumed to be stretched or compressed in the x (diagonal) direction. As a result, the vectors connecting next nearest-neighbor Cu ions in this layer have coordinates $\mathbf{d}'_1 = d(1 - \delta, 0)$ and $\mathbf{d}'_2 = d(0, 1)$, where parameter δ describes the strength of the stretching ($\delta < 0$) or compression ($\delta > 0$). The vectors connecting nearest-neighbor Cu ions of the layer 2 become $\mathbf{a}'_1 = (\mathbf{d}'_1 - \mathbf{d}'_2)/2$ and $\mathbf{a}'_2 = (\mathbf{d}'_1 + \mathbf{d}'_2)/2$. The positions of copper and oxygen ions in the layer 2 are

$$\begin{aligned} \mathbf{r}_{2\mathbf{n}}^d &\equiv \mathbf{r}_{2\mathbf{n}} = n\mathbf{a}'_1 + m\mathbf{a}'_2, \\ \mathbf{r}_{2\mathbf{n}}^{p_x} &= \mathbf{r}_{2\mathbf{n}} + \frac{1}{2}\mathbf{a}'_1, \quad \mathbf{r}_{2\mathbf{n}}^{p_y} = \mathbf{r}_{2\mathbf{n}} + \frac{1}{2}\mathbf{a}'_2. \end{aligned} \quad (3)$$

For a rational value of $1 - \delta = N_1/N_2$ (N_1 and N_2 are co-prime positive integers), the system has a superstructure. To satisfy the periodicity conditions, we must include two adjacent chains of copper and oxygen ions into superlattice cell aligned in the diagonal (x) direction. As a result, the superlattice cell will contain $2N_1$ copper ions of layer 1 and $2N_2$ copper ions of layer 2. It also will contain $4N_1$ oxygen ions of layer 1 and $4N_2$ oxygen ions of layer 2. The superlattice vectors are $\mathbf{R}_1 = N_1\mathbf{d}_1 = N_2(1 - \delta)\mathbf{d}_1$ and $\mathbf{R}_2 = 2\mathbf{d}_2$. The superlattice Brillouin zone (reduced Brillouin zone, RBZ) has

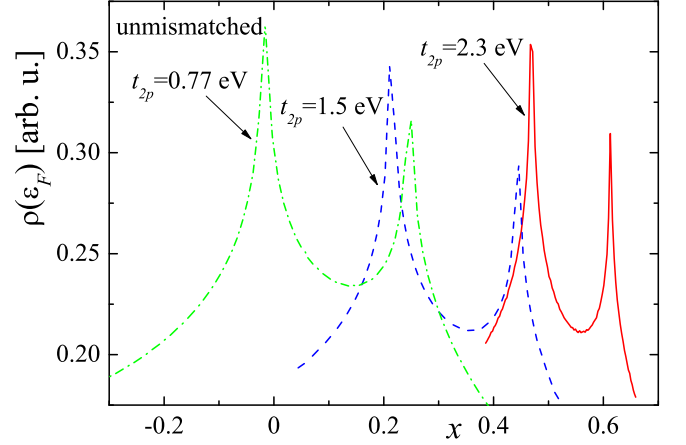


FIG. 2: Densities of states for unmismatched layers, calculated for three different values of t_{2p} . Other model parameters are: $\epsilon_{x^2-y^2} = 0$, $\epsilon_{p_x} = \epsilon_{p_y} = -0.9 \text{ eV}$, $\epsilon_a = 6.5 \text{ eV}$, $t_{1p} = 1.6 \text{ eV}$, $t_0 = 0.27 \text{ eV}$, and $t_0^{aa} = 0.75 \text{ eV}$. In order to avoid logarithmic singularities, the densities of states are averaged over the energy range $\Delta E = 7 \text{ meV}$.

a shape of the rectangle with the size $2\pi/(N_1d)$ in the x direction and $2\pi/d$ the y direction (see the right panel of Fig. 1).

III. TIGHT-BINDING MODEL OF MISMATCHED CuO_2 BILAYER

To describe electronic properties of mismatched CuO_2 bilayer, we use four-band tight-binding model. The model includes two types of p oxygen orbitals: p_x orbitals of oxygen ions located in positions $\mathbf{r}_{1\mathbf{n}}^{p_x}$ and p_y orbitals of oxygen ions located in positions $\mathbf{r}_{1\mathbf{n}}^{p_y}$. Model also includes two types of d orbitals of copper located in positions $\mathbf{r}_{1\mathbf{n}}^d$: these are $x^2 - y^2$ and ‘axial’ (a) orbitals. We do not specify here the nature of the latter a orbital, and only mention its circular symmetry in xy plane. It can be, e.g., s or $3z^2 - r^2$ orbital of copper, or their superposition. We include this orbital into the model because it gives the largest effect into interlayer hybridization⁵².

The Hamiltonian under study can be written as

$$H = H_1 + H_2 + H_{12}. \quad (4)$$

The terms $H_{1,2}$ correspond to each individual layer, while H_{12} describes the interlayer hybridization. Let us consider first intralayer terms. We use the simplest intralayer tight-binding Hamiltonian including only nearest neighbor hoppings of electrons between nearest copper and oxygen ions. The Hamiltonian H_i ($i = 1, 2$) reads

$$H_i = \sum_{\mathbf{n}A\sigma} \epsilon_A d_{\mathbf{n}iA\sigma}^\dagger d_{\mathbf{n}iA\sigma} + \sum_{\substack{(\mathbf{nm}) \\ d\sigma}} (t_{i\mathbf{nm}}^{dp} d_{\mathbf{n}id\sigma}^\dagger d_{\mathbf{m}ip\sigma} + H.c.), \quad (5)$$

where the subscript $A = \{d, p\}$ (with $d = x^2 - y^2$, a and $p = p_x, p_y$) denotes the considered orbitals, and $d_{\mathbf{n}iA\sigma}^\dagger$

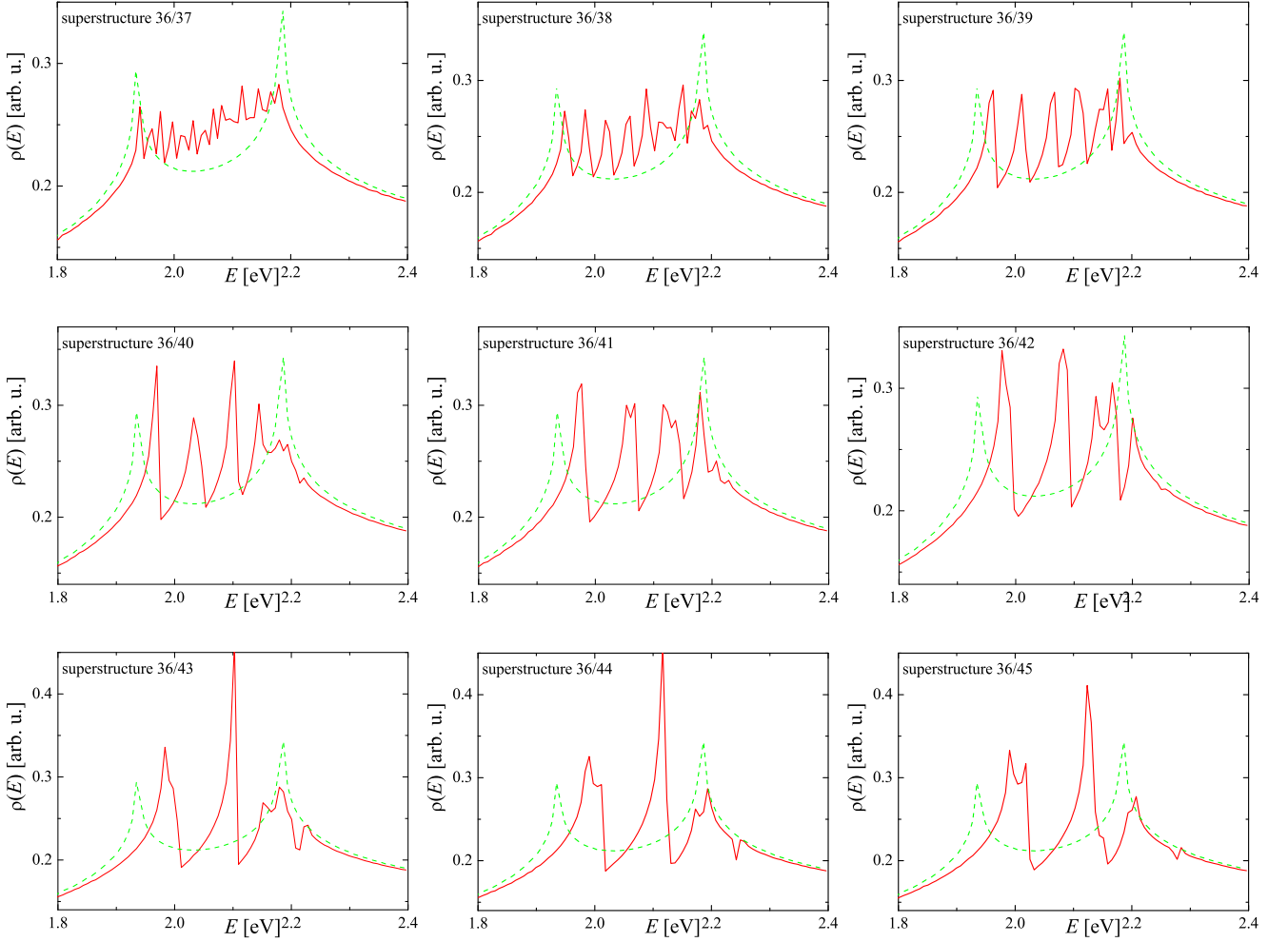


FIG. 3: Densities of states as functions of energy calculated for nine superstructures with $N_1 = 36$ and N_2 varying from 37 to 45. Model parameters correspond to Fig. 2 with $t_{2p} = 1.5$ eV. In order to avoid logarithmic singularities, the densities of states are averaged over the energy range $\Delta E = 7$ meV. The dashed green curve in each plot corresponds to unmismatched layers.

and $d_{\mathbf{n}iA\sigma}$ are the creation and annihilation operators of electron located in unit cell \mathbf{n} of layer i having orbital index A and spin projection σ . The first term in (5) includes the local energies of electrons in different orbitals, while the last term describes the nearest-neighbor hopping. The hopping amplitudes $t_{i\mathbf{n}\mathbf{m}}^{dp}$ are position dependent. For a given direction of hopping $\mathbf{n} \rightarrow \mathbf{m}$, the hopping amplitudes $t_{i\mathbf{n}\mathbf{m}}^{dp}$ can be written in the form of 2×2 matrix. The relationships between elements of this matrix can be easily obtained from the symmetry analysis of orbitals' wave functions⁵³. Let us introduce the Fourier transformed electron operators $d_{\mathbf{k}iA\sigma}$ and Fourier transformed hopping amplitudes $t_{i\mathbf{k}}^{dp}$. Taking into account the symmetry of the orbitals under study⁵³, one can write for layer 1

$$t_{1\mathbf{k}}^{dp} = \begin{pmatrix} -t_{1p}e^{-i\mathbf{k}\mathbf{a}_1/2} & t_{1p}e^{-i\mathbf{k}\mathbf{a}_2/2} \\ -t_{2p}e^{-i\mathbf{k}\mathbf{a}_1/2} & -t_{2p}e^{-i\mathbf{k}\mathbf{a}_2/2} \end{pmatrix}, \quad (6)$$

where we introduce two independent Slater-Koster parameters describing the hopping between $x^2 - y^2$ and p

orbitals (t_{1p}) and between a and p orbitals (t_{2p}). The similar formula for the layer 2 can be obtained from Eq. (6) with the change $\mathbf{a}_{1,2} \rightarrow \mathbf{a}'_{1,2}$. Strictly speaking, the values of parameters t_{1p} and t_{2p} for layer 2 are different from those for layer 1. In further analysis, however, we neglect this difference due to the smallness of the lattice distortion. Following Ref. 52, we use the following values of the tight-binding parameters: $\varepsilon_{x^2-y^2} = 0$, $\varepsilon_{p_x} = \varepsilon_{p_y} = -0.9$ eV, $t_{1p} = 1.6$ eV, $t_{2p} = 1.5$ eV. In our simulations, we use different values of the parameter ε_a describing the on-site energy of a orbital, taking both negative (almost $3z^2 - r^2$ orbital) and positive (almost s orbital) values. We also performed simulations for different values of the parameter t_{2p} describing hybridization between $x^2 - y^2$ orbitals of copper and p oxygen orbitals. Independent on the values of ε_a and t_{2p} , the density of states of individual layer has only one van Hove peak corresponding to the change of the Fermi surface topology. The position of this peak depends on ε_a and t_{2p} . In present study, we always focus on the energy range close

to the van Hove peak. The obtained results are similar for different values of ε_a and t_{2p} .

Let us consider now the interlayer hopping. According to Ref. 52, the largest interlayer hopping amplitudes are between a orbitals in two different layers, and between a and $p_{x,y}$ orbitals of different layers. As a result, Hamiltonian H_{12} takes the form

$$H_{12} = \sum_{\mathbf{nm}p\sigma} \left(t_{\perp\mathbf{nm}}^{ap} d_{\mathbf{n}2a\sigma}^\dagger d_{\mathbf{m}1p\sigma} + t_{\perp\mathbf{nm}}^{pa} d_{\mathbf{n}2p\sigma}^\dagger d_{\mathbf{m}1a\sigma} \right) + \sum_{\mathbf{nm}\sigma} t_{\perp\mathbf{nm}}^{aa} d_{\mathbf{n}2a\sigma}^\dagger d_{\mathbf{m}1a\sigma} + H.c. \quad (7)$$

The value of hopping amplitude depends on the mutual positions of two orbitals. In our simulations, we tried different parametrizations of interlayer hopping amplitudes depending on the possible symmetry of a orbital and obtain qualitatively similar results. If a orbital is assumed to be rather of s symmetry, the amplitude $t_{\perp\mathbf{nm}}^{ap_{x,y}}$ of electron hopping from oxygen ion in layer 1 located in the position $\mathbf{r}_{1\mathbf{m}}^{p_{x,y}}$ to copper ion in layer 2 located in the position $\mathbf{r}_{2\mathbf{n}}^d$ is described by the following Slater–Koster formula

$$t_{\perp\mathbf{nm}}^{ap_{x,y}} = \frac{(\mathbf{r}_{2\mathbf{n}}^d - \mathbf{r}_{1\mathbf{m}}^{p_{x,y}}) \mathbf{e}_{x,y}}{\sqrt{c^2 + (\mathbf{r}_{2\mathbf{n}}^d - \mathbf{r}_{1\mathbf{m}}^{p_{x,y}})^2}} V_\sigma(\mathbf{r}_{2\mathbf{n}}^d - \mathbf{r}_{1\mathbf{m}}^{p_{x,y}}), \quad (8)$$

where $\mathbf{e}_{x,y}$ is the unit vector in the direction of $\mathbf{a}_{1,2}$ and the function

$$V_\sigma(r) = t_0 \sqrt{1 + 8c^2/d^2} e^{-\frac{r - \sqrt{c^2 + d^2/8}}{r_0}}. \quad (9)$$

In the expression above, t_0 is the largest interlayer hopping amplitude between a and p orbitals, c is the interlayer distance (we choose $c = 3.35 \text{ \AA}$), and the parameter r_0 defines how fast the function $V_\sigma(r)$ decays with the distance between orbitals (we choose $r_0/d = 0.19$). Following Ref. 52, we take $t_0 = 0.27 \text{ eV}$. For the hopping amplitude between a orbitals in different layers, we have

$$t_{\perp\mathbf{nm}}^{aa} = V_0(\mathbf{r}_{2\mathbf{n}}^d - \mathbf{r}_{1\mathbf{m}}^d), \quad V_0(\mathbf{r}) = t_0^{aa} e^{-\frac{r - c}{r_0^{aa}}}, \quad (10)$$

where we choose $t_0^{aa} = 0.75 \text{ eV}$ and $r_0^{aa}/d = 0.3$.

Following the Slater–Koster formalism⁵³, we tried also a bit complicated parametrization of interlayer hopping amplitudes, which corresponds to a orbital rather of $3z^2 - r^2$ symmetry. Again, the functions similar to $V_\sigma(r)$ and $V_0(r)$, contain factors depending on directional cosines and the factors describing exponential decay with the distance between ions, but now the hopping amplitudes contain larger number of such functions. Details of this parametrization can be found elsewhere. Here, we present the results corresponding to the first parametrization, but let us notice again that qualitatively the results are independent of the type of the hopping amplitude parametrization.

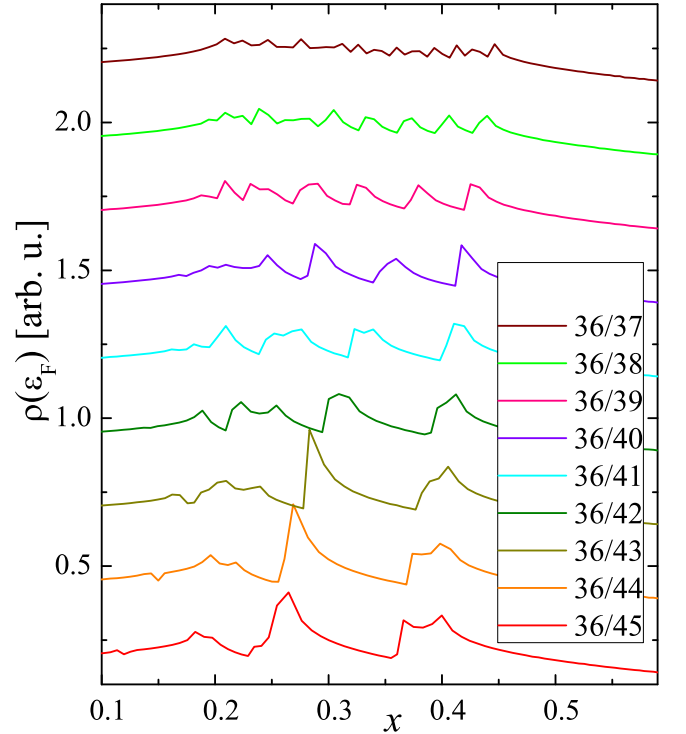


FIG. 4: Densities of states at Fermi level as functions of doping calculated for nine superstructures with $N_1 = 36$ and N_2 varying from 37 to 45. Model parameters correspond to Fig. 2 with $t_{2p} = 1.5 \text{ eV}$. In order to avoid logarithmic singularities, the densities of states are averaged over the energy range $\Delta E = 7 \text{ meV}$.

IV. RESULTS

Here, we demonstrate the evolution of the density of states and energy spectra for bilayers at different values of the lattice mismatch. We consider the superstructures with fixed $N_1 = 36$ and different N_2 ranging from $N_2 = 36$ (no mismatch) to $N_2 = 45$ (compressive strain). We suggest that apical orbital a is rather of s orbital of copper, so its energy level lays above $x^2 - y^2$ orbital, and $\varepsilon_a = 6.5 \text{ eV}$. In this case, the undoped bilayer has 5 electrons inside elementary unit cell of each layer (four electrons on $p_{x,y}$ orbitals plus one electron on $d_{x^2-y^2}$ orbital). We are interesting in the hole doped bilayers with doping $0 < x = 5 - n < 1$, where n is the number of electrons per CuO_2 unit cell. In the interesting energy range, the density of states of the individual layer has one van Hove singularity. For un-mismatched layers, the interlayer hopping terms split this van Hove singularity into two. Their energy positions depend on the model parameters. Thus, increasing the hopping amplitude between a and $p_{x,y}$ orbitals, t_{2p} , shifts these peaks to larger energies (smaller doping) in agreement with Ref. 54. For example, in Fig. 2 we show the densities of states at Fermi level as functions of doping x calculated for three different values of t_{2p} . Below, we consider the case of $t_{2p} = 1.5 \text{ eV}$ as

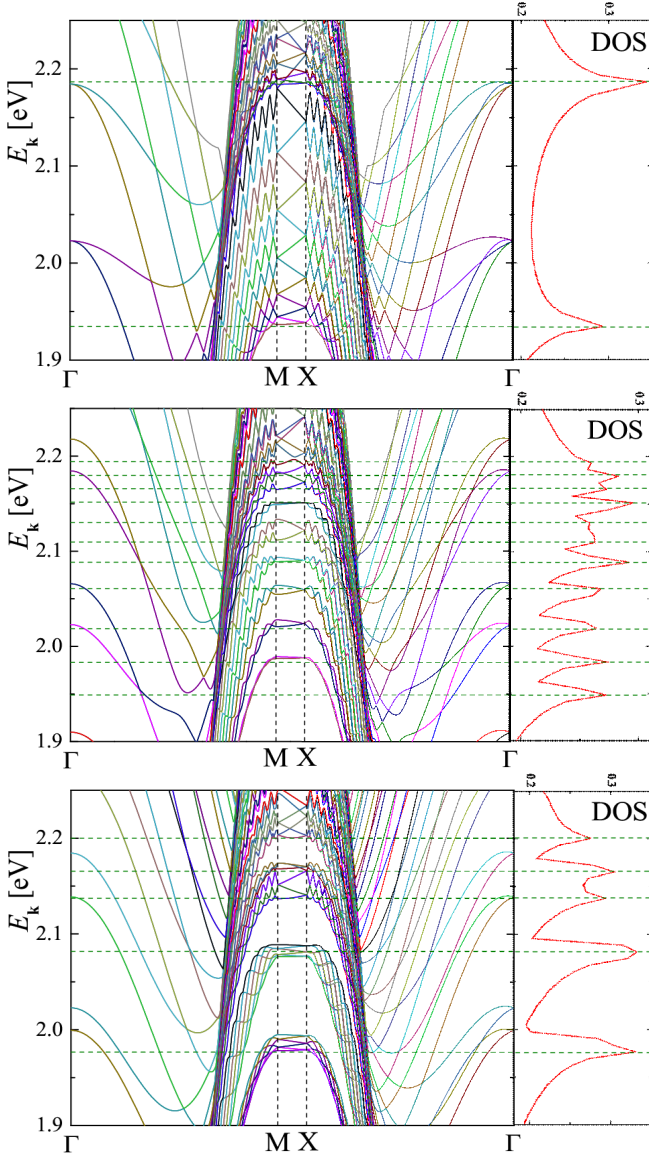


FIG. 5: Energy spectra calculated for superstructures with $N_1 = 36$ and $N_2 = 36$ (top panel, no mismatch), $N_2 = 38$ (middle panel), and $N_2 = 42$ (bottom panel). The spectra are calculated along the contour shown in Fig. 1. The distance between M and X points is enhanced by factor 5 for better view. Model parameters correspond to Fig. 2 with $t_{2p} = 1.5$ eV.

more realistic from the viewpoint of the positions of van Hove singularities in real compounds.

The main message of our work is that the mismatch between two CuO_2 layers generates extra van Hove singularities. For example, in Fig. 3, we show the densities of states as function of energy calculated for nine superstructures with $N_1 = 36$ and N_2 varying from 37 to 45. We clearly see extra van Hove singularities approximately located between to peaks corresponding to unmismatched layers. It is interesting, that the number of these extra van Hove singularities exhibits a contrintuitive be-

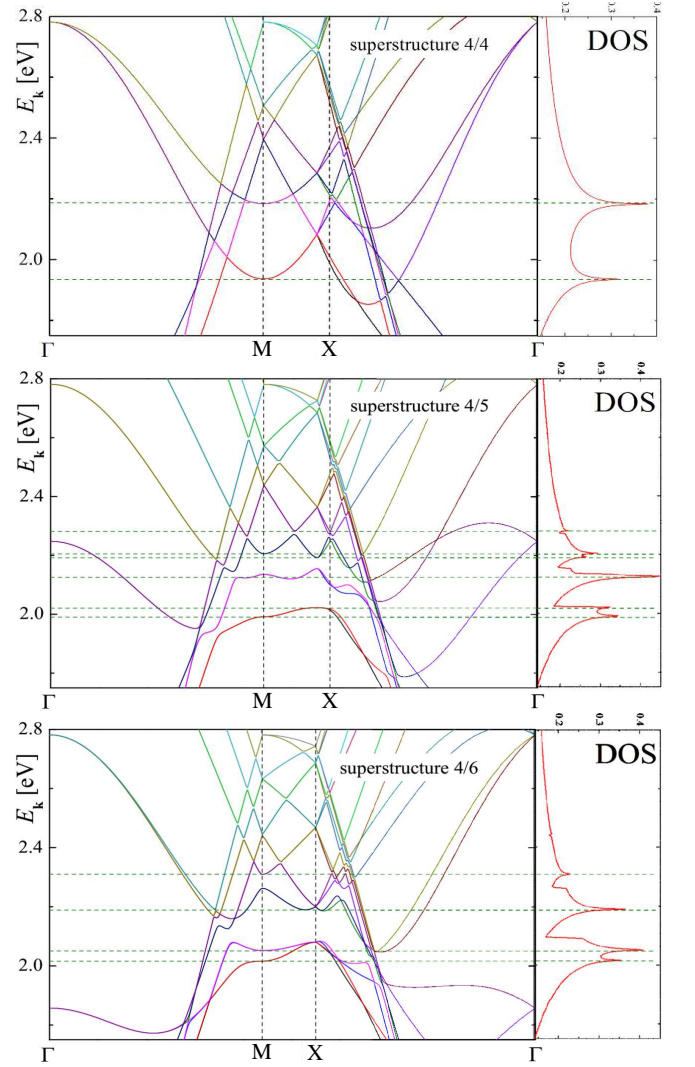


FIG. 6: Energy spectra calculated for superstructures with $N_1 = 4$ and $N_2 = 4$ (top panel, no mismatch), $N_2 = 5$ (middle panel), and $N_2 = 6$ (bottom panel). The spectra are calculated along the contour shown in Fig. 1. Model parameters correspond to Fig. 2 with $t_{2p} = 1.5$ eV.

havior with the change of N_2 : the number of peaks increases when N_2 decreases from $N_2 = 45$ to $N_2 = 37$. For better comparison, we show in a single plot, Fig. 4, the densities of states at Fermi level as functions of doping calculated for all nine superstructures with different N_2 and fixed $N_1 = 36$.

For better understanding of the origin of the extra van Hove singularities, we calculated the energy spectra for several superstructures (see Fig. 5). The spectra are calculated along the triangular contour connecting the most symmetrical points Γ , M , and X of the reduced Brillouin zone, see the right panel of Fig. 1. There are a lot of bands (about 100) inside the energy range shown, $1.9 \text{ eV} < E < 2.25 \text{ eV}$. This energy range includes two van Hove singularities of unmismatched layers (up-

per panel of Fig. 5), located at $E_{vHs}^1 \cong 1.93\text{eV}$ and $E_{vHs}^2 \cong 2.19\text{eV}$. The analysis shows that the origin of these two van Hove singularities are two saddle points of certain bands located at M point of the reduced Brillouin zone. In the energy range approximately between E_{vHs}^1 and E_{vHs}^2 , the band crossing occurs in the region near the line connecting M and X points of the RBZ, as it can be seen in top panel of Fig. 5. Such a picture is observed for unmismatched layers. When the layer 2 becomes stretched or compressed in comparison to layer 1, we observe a band flattening and band splitting in the region near the line connecting M and X points as it is seen in middle and bottom panels in Fig. 5. This band flattening gives rise to extra van Hove singularities with energies lying approximately between E_{vHs}^1 and E_{vHs}^2 . Situation here is very similar to that observed in twisted bilayer graphene², where the band flattening is observed for large superstructures, when the twist angle θ decreases down to critical value $\theta_c \sim 1^\circ$, while the moiré period increases as $L \propto 1/\theta$. In our case, however, the band flattening occurs only in the k_x -direction, since the band folding is performed only in this direction in the momentum space. As we can see from Fig. 5, the bands remain dispersive in the k_y -direction.

The spectra shown in Fig. 5 contain a lot of bands. For better illustration, we calculated also spectra for much smaller superlattices. Namely, we calculated spectra for superstructures with $N_1 = 4$ and $N_2 = 4, 5$, and 6 , see Fig. 6. Since, in these cases, the superlattice cell contains much smaller number of atoms, the energy range of interest (approximately between E_{vHs}^1 and E_{vHs}^2) contains much smaller number of bands. For superstructure with $N_1 = 4$ and $N_2 = 4$ (no mismatch, top panel of Fig. 6), we see two parabolic bands with minima at M points producing two van Hove singularities at energies E_{vHs}^1 and E_{vHs}^2 . By calculating the spectrum around small circle centred at M point, we have checked that M point is indeed a saddle point for corresponding bands. In the momentum range near the line connecting M and X points, we see several band crossings. When we compress layer 2 (superstructures with $N_2 = 4$ and 5 , middle and bottom panels in Fig. 6), this produces the band splittings, which give rise to extra van Hove singularities.

V. CONCLUSIONS

In conclusion, we have studied the model of double-layer BSCCO cuprate superconductor with mismatched

CuO₂ bilayers in diagonal direction. The mismatch between two layers produces the superstructure in the system. This gives rise to several extra van Hove singularities located approximately between energies E_{vHs}^1 and E_{vHs}^2 corresponding to two van Hove singularities of unmismatched layers. The number of these peaks and their energy positions depends on the quasi-commensurate superstructures of the *devil's staircase* in strained bilayers.

We have found that these extra van Hove singularities are closely related to the flattening and splitting of the bands inside the reduced Brillouin zone of unmismatched layers. The effect of the band flattening is similar to that observed in twisted bilayer graphene², where the large Fermi velocity reduction occurs for superstructures with small twist angles^{55,56}. In our case, however, the band flattening appears not in the whole Brillouin zone, but only in the direction of the band folding (k_x -direction). In the perpendicular direction, the bands remain dispersive.

The present results show that BSCCO is an intrinsic multi-band system where at high doping the chemical potential is close to a Lifshitz transition appearing at VHS at the metal to superconductor transition. Therefore, superconductivity in BSCCO is not a single-band unconventional superconducting phase but a multi-gap superconductor at a shape resonance described by Perali *et al.* in cuprates^{57,58} and appearing in diborides⁵⁹, oxide interfaces⁶⁰ and in room temperature hydride superconductors⁶¹.

In the optimum and overdoped regime, the position the Fermi level with respect to the peaks can be controlled by the gate voltage, this makes mismatched bilayer cuprates to be an efficient tool for fine tuning of the peaks of the electron density of states with respect to the Fermi level. Note that this effect is the most pronounced at rather small lattice mismatch, which produces numerous additional peaks in the density of states.

Acknowledgments

A.O.S. acknowledge the support of the Russian Science Foundation (project No. 22-22-00464) in the part concerning numerical calculations. K.I.K. acknowledge the support of the Russian Science Foundation (project No. 20-62-46047) in the part concerning the data analysis. We are grateful to the Joint Supercomputer Center of the Russian Academy of Sciences (JSCC RAS) for the provided computational resources.

¹ Y. Liu, N. O. Weiss, X. Duan, H.-C. Cheng, Y. Huang, and X. Duan, "Van der Waals heterostructures and devices," *Nat. Rev. Mater.* **1**, 16042 (2016).

² A. V. Rozhkov, A. O. Sboychakov, A. L. Rakhmanov, and F. Nori, "Electronic properties of graphene-based bilayer systems," *Phys. Rep.* **648**, 1 (2016).

³ A. Weston, Y. Zou, V. Enaldiev, A. Summerfield, N. Clark, V. Zólyomi, A. Graham, C. Yelgel, S. Magorrian, M. Zhou, et al., "Atomic reconstruction in twisted bilayers of transition metal dichalcogenides," *Nat. Nanotechnol.* **15**, 592–597 (2020).

⁴ W.-M. Zhao, L. Zhu, Z. Nie, Q.-Y. Li, Q.-W. Wang, L.-G.

- Dou, J.-G. Hu, L. Xian, S. Meng, and S.-C. Li, “Moiré enhanced charge density wave state in twisted 1T-TiTe₂/1T-TiSe₂ heterostructures,” *Nat. Mater.* (2021), published online.
- ⁵ Q. Tong, H. Yu, Q. Zhu, Y. Wang, X. Xu, and W. Yao, “Topological mosaics in moiré superlattices of van der Waals heterobilayers,” *Nat. Phys.* **13**, 356–362 (2017).
 - ⁶ Y.-N. Ren, Y. Zhang, Y.-W. Liu, and L. He, “Twistronics in graphene-based van der Waals structures,” *Chin. Phys. B* **29**, 117303 (2020).
 - ⁷ Y. Krockenberger, A. Ikeda, and H. Yamamoto, “Atomic stripe formation in infinite-layer cuprates,” *ACS Omega* **6**, 21884 (2021).
 - ⁸ H. Park, J. Oh, B. Song, and B. Kang, “Structural suitability of GdFeO₃ as a magnetic buffer layer for GdBa₂Cu₃O_{7-x} superconducting thin films,” *Progr. Supercond. Cryog.* **23**, 14 (2021).
 - ⁹ S. D. Conradson, T. H. Geballe, C.-Q. Jin, L.-P. Cao, A. Gauzzi, M. Karppinen, G. Baldinozzi, W.-M. Li, E. Gilioli, J. M. Jiang, et al., “Nonadiabatic coupling of the dynamical structure to the superconductivity in YSr₂Cu_{2.75}Mo_{0.25}O_{7.54} and Sr₂CuO_{3.3},” *PNAS* **117**, 33099 (2020).
 - ¹⁰ L. Sederholm, S. D. Conradson, T. H. Geballe, C.-Q. Jin, A. Gauzzi, E. Gilioli, M. Karppinen, and G. Baldinozzi, “Extremely overdoped superconducting cuprates via high pressure oxygenation methods,” *Condens. Matter* **6** (2021).
 - ¹¹ H. Jang, S. Asano, M. Fujita, M. Hashimoto, D. H. Lu, C. A. Burns, C.-C. Kao, and J.-S. Lee, “Superconductivity-insensitive order at $q \sim 1/4$ in electron-doped cuprates,” *Phys. Rev. X* **7**, 041066 (2017).
 - ¹² A. Bianconi, N. L. Saini, A. Lanzara, M. Messori, T. Rossetti, H. Oyanagi, H. Yamaguchi, K. Oka, and T. Ito, “Determination of the local lattice distortions in the CuO₂ plane of La_{1.85}Sr_{0.15}CuO₄,” *Phys. Rev. Lett.* **76**, 3412 (1996).
 - ¹³ N. Saini, H. Oyanagi, T. Ito, V. Scagnoli, M. Filippi, S. Agrestini, G. Campi, K. Oka, and A. Bianconi, “Temperature dependent local Cu-O displacements from underdoped to overdoped La-Sr-Cu-O superconductor,” *Eur. Phys. J. B* **36**, 75 (2003).
 - ¹⁴ A. Bianconi, M. Lusignoli, N. L. Saini, P. Bordet, A. Kvick, and P. G. Radaelli, “Stripe structure of the CuO₂ plane in Bi₂Sr₂CaCu₂O_{8+y} by anomalous x-ray diffraction,” *Phys. Rev. B* **54**, 4310 (1996).
 - ¹⁵ A. Bianconi, N. L. Saini, T. Rossetti, A. Lanzara, A. Perali, M. Messori, H. Oyanagi, H. Yamaguchi, Y. Nishihara, and D. H. Ha, “Stripe structure in the CuO₂ plane of perovskite superconductors,” *Phys. Rev. B* **54**, 12018 (1996).
 - ¹⁶ D. Di Castro, G. Bianconi, M. Colapietro, A. Pifferi, N. Saini, S. Agrestini, and A. Bianconi, “Temperature dependent local Cu-O displacements from underdoped to overdoped La-Sr-Cu-O superconductor,” *Eur. Phys. J. B* **18**, 617 (2000).
 - ¹⁷ A. Bianconi, G. Bianconi, S. Caprara, D. D. Castro, H. Oyanagi, and N. L. Saini, “The stripe critical point for cuprates,” *J. Phys. : Condens. Matter* **12**, 10655 (2000).
 - ¹⁸ S. Agrestini, N. Saini, G. Bianconi, and A. Bianconi, “The strain of CuO₂ lattice: the second variable for the phase diagram of cuprate perovskites,” *J. Phys. A: Math. Gen.* **36**, 9133 (2003).
 - ¹⁹ G. Wieggers, “Misfit layer compounds: Structures and physical properties,” *Progress in Solid State Chemistry* **24**, 1 (1996).
 - ²⁰ T. Janssen, A. Janner, A. Looijenga-Vos, and P. de Wolff in, *International Tables for Crystallography, Mathematical, Physical and Chemical Tables*, E. Prince, ed. (Wiley, New York, 2004), vol. C of *IUCr Series*, chap. 9.8. Incommensurate and Commensurate Modulated Structures, 3rd ed.
 - ²¹ J. Etrillard, P. Bourges, and C. T. Lin, “Incommensurate composite structure of the superconductor Bi₂Sr₂CaCu₂O_{8+δ},” *Phys. Rev. B* **62**, 150 (2000).
 - ²² D. Grebille, H. Leligny, and O. Pérez, “Comment on Incommensurate composite structure of the superconductor Bi₂Sr₂CaCu₂O_{8+δ},” *Phys. Rev. B* **64**, 106501 (2001).
 - ²³ A. Bianconi, “On the Fermi liquid coupled with a generalized Wigner polaronic CDW giving high T_c superconductivity,” *Solid State Commun.* **91**, 1 (1994).
 - ²⁴ A. Beskrovnyy and Z. Jirák, “Structural modulation in Bi₂Sr₂Ca_{0.4}Y_{0.6}Cu₂O_{8+δ},” *J. Phys. Conf. Ser.* **340** (2012).
 - ²⁵ O. Pérez, H. Leligny, D. Grebille, J. M. Grenèche, P. Labbé, D. Groult, and B. Raveau, “Disorder phenomena in the incommensurate compound Bi_{2+x}Sr_{3-x}Fe₂O_{9+δ},” *Phys. Rev. B* **55**, 1236 (1997).
 - ²⁶ V. Sedykh, V. Shekhtman, I. Smirnova, B. Bagautdinov, E. Suvorov, and A. Dubovitskii, “About specific features of the structure modulation in the Bi-ferrate compounds isostructural with Bi₂Sr₂CaCu₂O₈,” *Physica C* **390**, 311 (2003).
 - ²⁷ S. Lambert, H. Leligny, and D. Grebille, “Three forms of the misfit layered cobaltite [Ca₂CoO₃][CoO₂]_{1.62}. A 4D structural investigation,” *J. Solid State Chem.* **160**, 322 (2001).
 - ²⁸ D. Grebille, H. Muguerra, O. Pérez, E. Guilmeau, H. Rous-selière, and R. Funahashi, “Superspace crystal symmetry of thermoelectric misfit cobalt oxides and predicted structural models,” *Acta Cryst. B* **63**, 373 (2007).
 - ²⁹ J.-Y. Kim, J.-I. Kim, S.-M. Choi, Y. Soo Lim, W.-S. Seo, and H. Jin Hwang, “Nanostructured thermoelectric cobalt oxide by exfoliation/restacking route,” *J. Appl. Phys.* **112**, 113705 (2012).
 - ³⁰ V. A. Gavrichkov, Y. Shan’ko, N. G. Zamkova, and A. Bianconi, “Is there any hidden symmetry in the stripe structure of perovskite high-temperature superconductors?,” *J. Phys. Chem. Lett.* **10**, 1840 (2019).
 - ³¹ A. R. Mazza, X. Gao, D. J. Rossi, B. L. Musico, T. W. Valentine, Z. Kennedy, J. Zhang, J. Lapano, V. Keppens, R. G. Moore, et al., “Searching for superconductivity in high entropy oxide Ruddlesden-Popper cuprate films,” *J. Vac. Sci. Tech. A* **40**, 013404 (2022).
 - ³² S. Kaneko, Y. Shimizu, K. Akiyama, T. Ito, M. Mitsuhashi, S. Ohya, K. Saito, H. Funakubo, and M. Yoshimoto, “Modulation derived satellite peaks in x-ray reciprocal mapping on bismuth cuprate superconductor film,” *Appl. Phys. Lett.* **85**, 2301 (2004).
 - ³³ N. Poccia, G. Campi, M. Fratini, A. Ricci, N. L. Saini, and A. Bianconi, “Spatial inhomogeneity and planar symmetry breaking of the lattice incommensurate supermodulation in the high-temperature superconductor Bi₂Sr₂CaCu₂O_{8+y},” *Phys. Rev. B* **84**, 100504 (2011).
 - ³⁴ N. Poccia, S. Y. F. Zhao, H. Yoo, X. Huang, H. Yan, Y. S. Chu, R. Zhong, G. Gu, C. Mazzoli, K. Watanabe, et al., “Spatially correlated incommensurate lattice modulations in an atomically thin high-temperature Bi_{2.1}Sr_{1.9}CaCu_{2.0}O_{8+y} superconductor,” *Phys. Rev. Materials* **4**, 114007 (2020).

- ³⁵ Yuxiao Zhang, C. Hu, Y.-X. Hu, L. Zhao, Y. Ding, X. Sun, A. J. Liang, Yinchao Zhang, S. He, D. Liu, et al., “In situ carrier tuning in high temperature superconductor $\text{Bi}_2\text{Sr}_2\text{CaCu}_2\text{O}_{8+\delta}$ by potassium deposition,” *Sci. Bul.* **61**, 1037 (2016).
- ³⁶ A. Bianconi and N. Poccia, “Superstripes and complexity in high-temperature superconductors,” *J. Supercond. Novel Magn.* **25**, 1403 (2012).
- ³⁷ A. Bianconi, S. D. Longa, M. Messori, I. Pettiti, M. Pompa, and A. Soldatov, “Structure of the different Cu sites in the corrugated CuO_2 plane in high T_c superconductors,” *Jpn. J. Appl. Phys.* **32**, 578 (1993).
- ³⁸ J. Alldredge, J. Lee, K. McElroy, M. Wang, K. Fujita, Y. Kohsaka, C. Taylor, H. Eisaki, P. Uchida, S. Hirschfeld, and J. Davis, “Evolution of the electronic excitation spectrum with strongly diminishing hole density in superconducting $\text{Bi}_2\text{Sr}_2\text{CaCu}_2\text{O}_{8+\delta}$,” *Nat. Phys.* **4**, 319 (2008).
- ³⁹ A. N. Pasupathy, A. Pushp, K. K. Gomes, C. V. Parker, J. Wen, Z. Xu, G. Gu, S. Ono, Y. Ando, and A. Yazdani, “Electronic origin of the inhomogeneous pairing interaction in the high- T_c superconductor $\text{Bi}_2\text{Sr}_2\text{CaCu}_2\text{O}_{8+\delta}$,” *Science* **320**, 196 (2008).
- ⁴⁰ K. K. Gomes, A. N. Pasupathy, A. Pushp, S. Ono, Y. Ando, and A. Yazdani, “Visualizing pair formation on the atomic scale in the high- T_c superconductor $\text{Bi}_2\text{Sr}_2\text{CaCu}_2\text{O}_{8+\delta}$,” *Nature* **447**, 569 (2007).
- ⁴¹ I. Božović, X. He, J. Wu, and A. Bollinger, “Dependence of the critical temperature in overdoped copper oxides on superfluid density,” *Nature* **536**, 309 (2016).
- ⁴² Y. He, S.-D. Chen, Z.-X. Li, D. Zhao, D. Song, Y. Yoshida, H. Eisaki, T. Wu, X.-H. Chen, D.-H. Lu, et al., “Superconducting fluctuations in overdoped $\text{Bi}_2\text{Sr}_2\text{CaCu}_2\text{O}_{8+\delta}$,” *Phys. Rev. X* **11**, 031068 (2021).
- ⁴³ I. K. Drozdov, I. Pletikosić, C.-K. Kim, K. Fujita, G. Gu, J. C. S. Davis, P. Johnson, I. Božović, and T. Valla, “Phase diagram of $\text{Bi}_2\text{Sr}_2\text{CaCu}_2\text{O}_{8+\delta}$ revisited,” *Nat. Commun.* **9**, 5210 (2018).
- ⁴⁴ X. Li, Y. Ding, C. He, W. Ruan, P. Cai, C. Ye, Z. Hao, L. Zhao, X. Zhou, Q. Wang, et al., “Quasiparticle interference and charge order in a heavily overdoped non-superconducting cuprate,” *New Journal of Physics* **20**, 063041 (2018).
- ⁴⁵ T. A. Maier, S. Karakuzu, and D. J. Scalapino, “Overdoped end of the cuprate phase diagram,” *Phys. Rev. Research* **2**, 033132 (2020).
- ⁴⁶ M.Yu. Kagan, K.I. Kugel, and A.L. Rakhmanov, “Electronic phase separation: Recent progress in the old problem,” *Phys. Rep.* **916**, 1 (2021).
- ⁴⁷ A. L. Rakhmanov, K. I. Kugel, M. Yu. Kagan, A. V. Rozhkov, and A. O. Sboychakov, “Inhomogeneous electron states in the systems with imperfect nesting,” *JETP Letters* **105**, 806 (2017).
- ⁴⁸ K. I. Kugel, A. L. Rakhmanov, A. O. Sboychakov, N. Poccia, and A. Bianconi, “Model for phase separation controlled by doping and the internal chemical pressure in different cuprate superconductors,” *Phys. Rev. B* **78**, 165124 (2008).
- ⁴⁹ A. Bianconi, N. Poccia, A. O. Sboychakov, A. L. Rakhmanov, and K. I. Kugel, “Intrinsic arrested nanoscale phase separation near a topological Lifshitz transition in strongly correlated two-band metals,” *Supercond. Sci. Technol.* **28**, 024005 (2015).
- ⁵⁰ K. I. Kugel, A. L. Rakhmanov, A. O. Sboychakov, F. V. Kusmartsev, N. Poccia, and A. Bianconi, “A two-band model for the phase separation induced by the chemical mismatch pressure in different cuprate superconductors,” *Supercond. Sci. Technol.* **22**, 014007 (2008).
- ⁵¹ P. Bak, “Commensurate phases, incommensurate phases and the devil’s staircase,” *Rep. Prog. Phys.* **45**, 587 (1982).
- ⁵² O. Andersen, A. Liechtenstein, O. Jepsen, and F. Paulsen, “LDA energy bands, low-energy Hamiltonians, t' , t'' , $t_\perp(k)$, and J_\perp ,” *J. Phys. Chem. Solids* **56**, 1573 (1995).
- ⁵³ J. C. Slater and G. F. Koster, “Simplified LCAO method for the periodic potential problem,” *Phys. Rev.* **94**, 1498 (1954).
- ⁵⁴ E. Pavarini, I. Dasgupta, T. Saha-Dasgupta, O. Jepsen, and O. K. Andersen, “Band-Structure Trend in Hole-Doped Cuprates and Correlation with T_{cmax} ,” *Phys. Rev. Lett.* **87**, 047003 (2001).
- ⁵⁵ J. M. B. Lopes dos Santos, N. M. R. Peres, and A. H. Castro Neto, “Continuum model of the twisted graphene bilayer,” *Phys. Rev. B* **86**, 155449 (2012).
- ⁵⁶ A. O. Sboychakov, A. L. Rakhmanov, A. V. Rozhkov, and F. Nori, “Electronic spectrum of twisted bilayer graphene,” *Phys. Rev. B* **92**, 075402 (2015).
- ⁵⁷ A. Perali, A. Bianconi, A. Lanzara, and N. L. Saini, “The gap amplification at a shape resonance in a superlattice of quantum stripes: A mechanism for high T_c ,” *Solid State Commun.* **100**, 181 (1996).
- ⁵⁸ A. Perali, D. Innocenti, A. Valletta, and A. Bianconi, “Anomalous isotope effect near a 2.5 Lifshitz transition in a multi-band multi-condensate superconductor made of a superlattice of stripes,” *Supercond. Sci. Technol.* **25**, 124002 (2012).
- ⁵⁹ S. Agrestini, C. Metallo, M. Filippi, L. Simonelli, G. Campi, C. Sanipoli, E. Liarokapis, S. De Negri, M. Giovannini, A. Saccone, et al., “Substitution of Sc for Mg in MgB_2 : Effects on transition temperature and Kohn anomaly,” *Phys. Rev. B* **70**, 134514 (2004).
- ⁶⁰ A. Bianconi, D. Innocenti, A. Valletta, and A. Perali, “Shape resonances in superconducting gaps in a 2DEG at oxide-oxide interface,” *J. Phys. Conf. Ser.* **529**, 012007 (2014).
- ⁶¹ M. V. Mazziotti, R. Raimondi, A. Valletta, G. Campi, and A. Bianconi, “Resonant multi-gap superconductivity at room temperature near a Lifshitz topological transition in sulfur hydrides,” *J. Appl. Phys.* **130**, 173904 (2021).